International Journal of Biological Macromolecules 165 (2020) 738–746

Contents lists available at ScienceDirect

International Journal of Biological Macromolecules

journal homepage: http://www.elsevier.com/locate/ijbiomac

Degradation models, structure, rheological properties and protective effects on erythrocyte hemolysis of the polysaccharides from *Ribes nigrum* L

Haihong Yang [1], Jingwen Bai [1], Conglei Ma, Libo Wang, Xiaoqing Li, Yu Zhang, Yaqin Xu *, Yu Yang *

College of Art and Science, Northeast Agricultural University, Harbin 150030, China

ARTICLE INFO

Article history:
Received 5 July 2020
Received in revised form 5 September 2020
Accepted 14 September 2020
Available online 21 September 2020

Keywords:
Blackcurrant polysaccharide
Ultrasonic treatment
Degradation model
Rheological properties
Structure
Erythrocyte hemolysis

ABSTRACT

The polysaccharides from blackcurrant (*Ribes nigrum* L.) fruits were degraded by ultrasonic irradiation. Results showed that viscosity-average molecular weight decreased with increasing ultrasonic time or power. The degradation was fitted to the second-order kinetics model and midpoint chain scission model. Gas chromatographic analysis demonstrated that the native polysaccharide and three degraded polysaccharides were composed of the same monosaccharides but in different ratios. Fourier transform infrared and nuclear magnetic resonance spectroscopic analyses revealed the presence of α-, β-pyranose rings and the same six sugar residues in the four blackcurrant polysaccharides. Compared to the native polysaccharide, three degraded polysaccharides displayed better rheological properties and stronger protective effects against erythrocyte hemolysis. Collectively, the results support the potential utility of blackcurrant polysaccharides as natural antioxidants.

© 2020 Elsevier B.V. All rights reserved.

1. Introduction

Blackcurrant (*Ribes nigrum* L.) fruit is a small, dark-purple berry that is widely applied to produce jams, wines and juices [1]. Blackcurrant is also healthy and contains many beneficial substances including anthocyanins, flavonols, phenolic acid, polysaccharides, vitamins and organic acids [1,2]. Previous findings have demonstrated that blackcurrant fruits possess various beneficial effects on human health, such as hypoglycemic, antiviral, antimicrobial and anti-cancer effects [3,4]. Polysaccharides, as one of the main active components in blackcurrant, are claimed to possess immunoregulatory, antioxidant, anti-tumor, antiviral and hypoglycemic capacities, etc. [1,5,6]. Our previous research revealed that blackcurrant polysaccharides exhibited the high molecular weight and low water solubility [7], which influenced their bioactivities and utilization in vivo. It is considered that the polysaccharides with larger molecular weight are very hard to span multiple cell membrane into tissues to take effects [8]. Moreover, several literature has proved that the low-molecular-weight polysaccharides always possess better bioactivities, making them more useful in the medicine and food industry [7–9]. Consequently, it is important to establish an effective, rapid and green technique for polysaccharides degradation to increase their physiological activities and expand the applications in the food and pharmaceutical industries.

At present, the techniques proposed for polysaccharides degradation mainly include chemical degradation, physical degradation and enzymatic hydrolysis [8,10]. Chemical methods (e.g., oxidation and acid hydrolysis) have some shortcomings including high environmental pollution and complicated post-treatment [9,11]. Enzymatic degradation requires the use of various high-cost enzymes, limiting their industrial application [9,12]. Reported methods for physical degradation include ultrasound [10], microwave [13], thermal treatment [14], and gamma irradiation [15]. Among them, the ultrasonic degradation has gained considerable attention in recent years because it is a rapid, mild and environment-friendly technique that can improve the bioactivities of the polysaccharides with only minor structural destruction [10,12,16].

In our previous study, blackcurrant polysaccharides obtained by hot-water extraction were degraded using the ultrasonic irradiation at power of 400 and 600 W, and the treatment of Fe^{2+}-H_2O_2 at two concentrations. These studies revealed that the degradation treatment reduced the molecular weight of blackcurrant polysaccharides and improved the biological activities of the crude polysaccharides, while the basic structure of the polysaccharides was not changed [5,7]. However, the degradation kinetics model and chain scission model of blackcurrant polysaccharides were not evaluated. The establishment of the degradation kinetics model is important for the preparation of the polysaccharides with the desired molecular weight. In addition, chemiluminescence method was used to evaluate the antioxidant

* Corresponding authors.
E-mail addresses: xuyaqin@neau.edu.cn (Y. Xu), yangyu@neau.edu.cn (Y. Yang).
[1] These authors contributed equally to this work.

https://doi.org/10.1016/j.ijbiomac.2020.09.093
0141-8130/© 2020 Elsevier B.V. All rights reserved.

activities in these reports, which had limited accuracy. Recently, cell models have become a mainstream method to evaluate the antioxidant activity and reveal the action mechanism based on a realistic biological environment [17,18]. However, limited information is available for the polysaccharides from small berry fruits.

In this study, blackcurrant polysaccharides were extracted using complex enzymatic method and degraded by ultrasonic irradiation. The kinetics of the degradation, and the influences of ultrasonic power on the molecular weight, rheological properties and structure of the polysaccharides were systematically studied. In addition, the protection effects of the high-purity polysaccharides against erythrocyte hemolysis were assessed.

2. Materials and methods

2.1. Materials and reagents

The ripe fruits of blackcurrant (Heifeng) were acquired from Mudanjiang Institute of Agricultural Science (Mudanjiang, China). The samples were washed, packed under vacuum, and stored at −20 °C prior to use. A series of dextrans (T-10, T-40, T-70, T-110, T-500 and T-2000) were purchased from Baierdi Biotechnology Co. (Beijing, China). Dextran (T-3755) was provided by American Polymer Standards Corp. (Ohio, USA). Sephacryl S-500 was purchased from Shanghai Yuanye Biotechnology Co., Ltd. (Shanghai, China). Pectinase (1000 U/mg) and papain (500 U/mg) were purchased from Beijing Obo Star Biotechnology Co., Ltd. (Beijing, China). Rabbit erythrocyte was obtained from Guangzhou Hongquan Biotechnology Co., Ltd. (Guangzhou, China). Glutathione (GSH) and malondialdehyde (MDA) assay kits were purchased from Nanjing Building Technology Co., Ltd. (Nanjing, China). All other reagents were of analytical grade.

2.2. Preparation of the polysaccharides from blackcurrant fruits

A complex enzymatic method was used to extract the polysaccharides. Briefly, 20.0 g homogenate of blackcurrant fruits with a moisture content of 76.20% ± 0.62% was mixed with deionized water (400.0 mL), and then the complex enzymes including papain (60.0 mg) and pectinase (30.0 mg) were added to the mixture. The suspension was extracted at 50 °C for 50 min, and then the residue was removed by vacuum filtration. The supernatant was concentrated, and precipitated by the addition of anhydrous ethanol to a final concentration of 75.0% (v/v) and then kept at 4 °C overnight. The polysaccharide precipitate was obtained by vacuum filtration using a 0.45 μm filter paper. Subsequently, the crude polysaccharides were redissolved in distilled water, and purified with a D4006 macroporous resin according to our previous study [7]. The fraction containing the polysaccharides component was pooled, concentrated, and lyophilized to obtain the polysaccharides sample, which was designated as BP (blackcurrant polysaccharides) and used in the subsequent trials.

2.3. Degradation of the polysaccharides by ultrasonic irradiation

Ultrasonic degradation was performed in an ultrasonic cell crushing instrument (JY92-IIV, Ningbo Xinzhi Biotech Co., Ltd., Ningbo, China) with a maximum output power of 1000 W. Briefly, a 100 mL beaker containing 50 mL of BP solution (5.0 mg/mL) was immersed into an ice bath to keep solution at a temperature of 10 ± 2 °C, then ultrasound probe with 6 mm diameter was dipped into the solution with fixed depth of 2.0 cm in all experiments. Then BP solution was treated intermittently (1 s on, 1 s off) at different ultrasonic powers (300, 500 and 700 W) for different time periods (5, 10, 15, 20, 30, 40, 60, 80 and 100 min) to prepare degraded polysaccharides. The series of degraded polysaccharides solutions were concentrated, freeze-dried and used for standby.

2.4. Determination of intrinsic viscosity and viscosity-average molecular weight

The intrinsic viscosity [η] of the polysaccharides solution was assayed by an Ubbelohde viscometer at 25 ± 0.1 °C [19]. In brief, different concentrations of the polysaccharides were prepared. The relative viscosity(η_r) and specific viscosity (η_{sp}) were computed using following formulas (1) and (2), respectively. All the experimental sets were performed 3–5 times, and the reproducibility for the determination of efflux time was within 0.2 s. Subsequently, plots of η_{sp}/c against c (concentration of the polysaccharide solution) and $\ln\eta_r/c$ against c were drawn, and [η] of the polysaccharides was obtained from the intercept of a dual extrapolation [20].

$$\eta_r = \frac{t}{t_0} \tag{1}$$

$$\eta_{sp} = \eta_r - 1 \tag{2}$$

where, t and t_0 represent the efflux time for the polysaccharide solution and deionized water, separately.

The viscosity-average molecular weight (M_η) of the polysaccharide is related to its [η] by Mark-Houwink equation (shown in Eq. (3)). The values of the experience parameters (K and α) are decided by the type of polymer, solvent and temperature for viscosity assay. In this study, the intrinsic viscosity [η] of four dextran standard samples was obtained from the intercept of a dual extrapolation (Fig. S1). Subsequently, the curve of lg[η] versus lg$M$ was drawn (Fig. S2), where lg$K$ and α stand for the intercept and slope of the plot, separately. As a result, the values of K and α are 0.6446 and 0.3146, respectively.

$$[\eta] = KM_\eta^\alpha \tag{3}$$

2.5. Degradation models of the polysaccharides under ultrasonic irradiation

2.5.1. Degradation kinetics models

Graphical analysis was used to investigate the degradation kinetics models of the samples under different ultrasonic power. The first-order and second-order reaction kinetics models were used to estimate ultrasonic degradation behavior of the polysaccharides [21], which were expressed as Eqs. (4) and (5), respectively:

$$\ln\left(\frac{M_t}{M_0}\right) = -kt \tag{4}$$

$$\frac{1}{M_t} - \frac{1}{M_0} = kt \tag{5}$$

where k is the degradation rate constant (min^{-1} and $mol\cdot g^{-1}\cdot min^{-1}$, respectively); t is the treatment time (min); M_t and M_0 are viscosity-average molecular weight at time t and at time 0 (Da), separately.

2.5.2. Chain scission models

Midpoint chain scission (shown in Eq. (6)) and random chain scission (shown in Eq. (7)) were used to describe the behavior of chain scission of the polysaccharides under ultrasonic irradiation [22].

$$\ln\left(\frac{M_0 - M_{lim}}{M_t - M_{lim}}\right) = k_1 M_{lim} t \tag{6}$$

$$\frac{M_{lim}}{M_t} + \ln\left(1 - \frac{M_{lim}}{M_t}\right) = -\frac{k_2}{c} t\left(\frac{M_{lim}}{m}\right)^2 + \frac{M_{lim}}{M_0} + \ln\left(1 - \frac{M_{lim}}{M_0}\right) \tag{7}$$

where M_0, c represent molecular weight and concentration of the sample at time 0; M_t, M_{lim} and m are molecular weight at time t, the limiting

molecular weight, and the molecular weight of monomer, individually; k_1 and k_2 refer to the degradation rate constant.

2.6. Purification of the polysaccharides

The 1,1-diphenyl-2-picrylhydrazyl (DPPH) radical scavenging activities of a series of degraded polysaccharides were determined according to our previous report [7]. In view of DPPH radical scavenging abilities (data not be shown) and molecular weight of these degraded polysaccharides, the three degraded polysaccharides obtained by treatment at ultrasonic power of 300, 500 and 700 W for 60 min were selected for subsequent study.

BP and three degraded polysaccharides were purified by Sephacryl S^{-500} column (1.6 × 50 cm) chromatography. Briefly, the sample solution (1.0 mL, 10.0 mg/mL) was injected into the column, and then was eluted with deionized water at a flow rate of 0.8 mL/min. The collected eluant (1.0 mL/tube) was monitored using the phenol-sulfuric acid method [23]. The main fraction containing the polysaccharides was combined, concentrated, and lyophilized. Consequently, purified blackcurrant polysaccharides (PBP) and three degraded polysaccharides (U-300, U-500 and U-700) were obtained, respectively.

2.7. Physicochemical properties of the polysaccharides

2.7.1. Molecular weight analysis

The molecular weights of the polysaccharides were determined by high-performance liquid chromatography (HPLC) based on our previous study [6].

2.7.2. Calculation of the degradation degree

The degradation rate of the molecular weight was defined as Eq. (8) [24].

$$\text{Degradation rate} = \frac{M_{w0} - M_{wt}}{M_{w0}} \times 100\% \quad (8)$$

where M_{w0} and M_{wt} are the weight-average molecular weight at ultrasonic time 0 and at time t, respectively.

2.7.3. Chemical composition analysis

Total sugar content was quantitatively determined using the phenol-sulfuric acid means [23]. Uronic acid content was estimated through the carbazole-sulfuric acid method using D-galacturonic acid (GalA) as a standard [25]. Monosaccharide composition was detected on gas chromatography (GC, Shimadzu Corporation, Kyoto, Japan) fitted with a flame ionization detector and an RTX-1701 silica capillary column (30.0 m × 0.25 mm × 0.25 μm). The processes were employed as the described previously [26].

2.7.4. Rheological analysis

Rheological properties of PBP and the degraded products (U-300, U-500 and U-700) were evaluated using a Discovery HR-1 hybrid rheometer (TA Instruments, New Castle, USA) equipped with a cone-plate (60 mm diameter, 1 mm gap, 1° angle) at 25.0 ± 0.1 °C. Briefly, the polysaccharides solution (8.0 mg/mL, 7.0 mL) was moved to the plate and equilibrated for 10 min prior to the measurement. The apparent viscosity was measured under shear rate sweeping from 1 to 100 s^{-1}. Storage modulus (G') and loss modulus (G'') were evaluated with angular frequency (1 to 1000 rad/s) at 1% strain within linear viscoelastic region.

2.7.5. Fourier-transform infrared spectrometer (FT-IR) and nuclear magnetic resonance (NMR)

PBP and the degraded polysaccharides (U-300, U-500 and U-700) were ground with potassium bromide powder and then pressed into pellets for FT-IR spectroscopic analysis (ALPHA-T, Bruker Instruments, Ettlingen, Germany), The FT-IR spectra were recorded in the frequency range of 500–4000 cm^{-1}.

For NMR analysis, the polysaccharides were dissolved in D_2O (99.9%) and transferred into the NMR-tube. 1D-NMR (^1H NMR and ^{13}C NMR) spectra and 2D-NMR spectra including homonuclear correlation (COSY) and heteronuclear single quantum coherence (HSQC), were gained on an AVANCE III HD 500 MHz NMR spectrometer (Bruker Corporation, Zurich, Switzerland) at 25 °C.

2.8. Assays of hemolysis protection of erythrocyte

2.8.1. Hemolysis rate of erythrocyte induced by H_2O_2

The effects of the polysaccharides on H_2O_2- induced hemolysis were investigated based on the previous study [27]. Trolox was served as the control. The hemolysis inhibition rate was computed according to Eq. (9):

$$\text{Hemolysis inhibition rate} = \left(B - \frac{A_1}{A_0}\right) \times 100\% \quad (9)$$

where A_1 refers to the absorbance of the supernatant diluted by NaCl solution; A_0 refers to the absorbance of the supernatant diluted by distilled water; B represents the hemolysis rate induced by H_2O_2 (1.0 mmol/L) in the absence of the polysaccharides.

2.8.2. H_2O_2-induced GSH content in erythrocyte

GSH level was determined using a GSH assay kit according to the manufacturer's manual. When dinitrobenzoic acid was mixed with sulfhydryl compounds, a yellow compound was generated and assayed at 420 nm. Trolox was used as the control and GSH content was presented as gGSH/L.

2.8.3. H_2O_2-induced MDA content in erythrocyte

MDA level was detected adopting MDA kit in accordance with the instructions. MDA reacted with thiobarbituric acid (TBA) to generate red compounds, which were assayed at 532 nm. Trolox was served as the control.

2.9. Statistical analysis

All tests were conducted in triplicate and the data were presented as means ± standard deviation. The statistical analyses were done by SPSS 18.0 (SPSS Inc., Chicago, USA). A probability level of $P < 0.05$ was set to examine statistical significance for all tests.

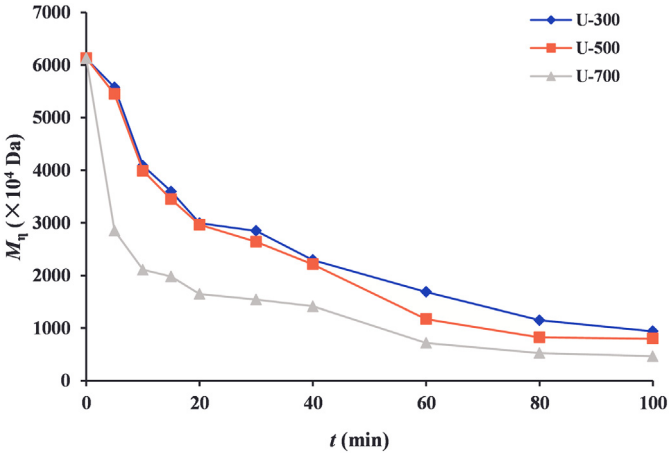


Fig. 1. Effect of ultrasonic irradiation on the M_η.

3. Results and discussion

3.1. Effect of ultrasonic irradiation on M_η

The M_η of the polysaccharides under different ultrasonic power as a function of time was depicted in Fig. 1. It was observed that the M_η under different ultrasonic power decreased with increasing ultrasonic time. For the same treatment time, the higher ultrasonic power corresponded to a smaller M_η. These results demonstrated that the ultrasonic power had an important effect on the degradation of blackcurrant polysaccharides. After ultrasonic treatment for 100 min, M_η decreased from 6.12×10^7 to 9.40×10^6, 8.00×10^6, and 4.65×10^6 Da under ultrasonic power of 300, 500 and 700 W, separately. Similarly, the molecular weight of the polysaccharides from *Phellinus linteus* mycelia and sea cucumber fucoidan decreased with increasing ultrasonic power [16,24]. In addition, the M_η decreased rapidly within the first 20 min of ultrasonic treatment the degradation rate was 73.04% at 700 W, but decreased slowly in the range of 20–100 min. Similar results were also obtained in ultrasonic treatment of other polysaccharides, including dextran [24], schizophyllan [21], apple pectin [28] and polysaccharides from *Phellinus linteus* mycelia [12]. The influence of ultrasonic irradiation on the degradation of the polysaccharides may be ascribed to cavitation action [12,16]. In a certain range, higher ultrasonic power increases cavitation energy and the quantity of cavitation bubbles, leading to the enhancement in efficiency of energy transmission into the reaction system [16,28]. Thus, an obvious decrease in M_η was observed with increasing ultrasonic power.

Table 1
Parameters of degradation models for BP under different ultrasonic power.

Ultrasonic power (W)	First-order degradation kinetic		Second-order degradation kinetic		Midpoint scission		Random scission	
	k	R^2	k	R^2	k	R^2	k	R^2
300	0.0201	0.966	0.1033	0.983	0.0390	0.983	0.0113	0.711
500	0.0263	0.986	0.1929	0.997	0.0508	0.982	0.0195	0.759
700	0.0309	0.979	0.2537	0.990	0.0564	0.989	0.0246	0.776

3.2. Degradation model analysis

3.2.1. Degradation kinetics models

To evaluate the degradation behavior of ultrasonic treatment on BP, kinetic curves of the first- and second-order reactions and related kinetics parameters are shown in Fig. 2A–B and Table 1. It is observed that ($1/M_t$-$1/M_0$) of second-order mathematical model for BP presented better linear relationship with treatment time under various ultrasonic power, and the correlation coefficient (R^2) was closer to 1. Thus, second-order mathematical model was more suitable to illustrate the degradation behavior of BP. In addition, as shown in Table 1, k elevated with the ultrasonic power increasing. This phenomenon may be related to the enhancement of cavitation, which ultimately provides more chance for the breakage of the polysaccharide chains [12]. It was reported that some polysaccharides such as *Phellinus linteus mycelia*

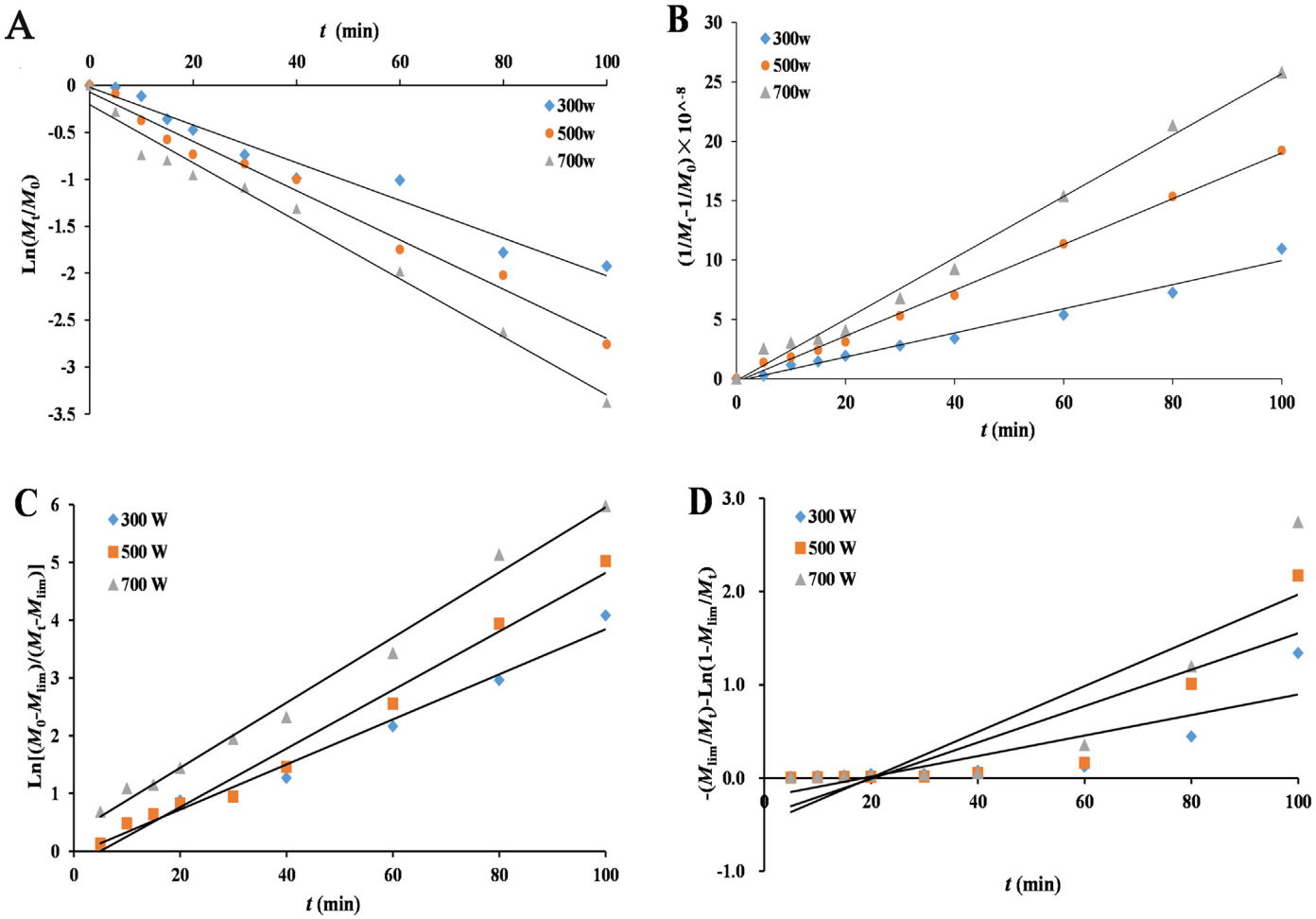


Fig. 2. The degradation model curves of BP under different ultrasonic powers. (A) First-order degradation kinetic model; (B) second-order degradation kinetic model; (C) midpoint scission model; and (D) random scission model.

polysaccharides [12] *Auricularia auricula* polysaccharide [10], apple pectin [28] and Schizophyllan [21] have also been found to follow second-order degradation kinetics under ultrasonic treatment.

3.2.2. Chain scission mode

In general, two simple models (midpoint and random fracture models) have been developed to describe the position of polymers chain fracture. Midpoint fracture model presumes that the chain fracture occurs in the center of the chain skeleton; in contrast, the random fracture model supposes the polymer breakage is random, and any chain linkage possesses the same fracture probability [22,24].

As shown in Fig. 2C–D, the plot of midpoint scission model presented better linear relationship than that of random scission model. Besides, the R^2 value of the midpoint scission model (>0.98) demonstrated that this model was more reasonable to describe the experimental data (Table 1). Thus, the ultrasonic degradation of BP occurred primarily through the midpoint scission. Similarly, the midpoint scission model was found to be more appropriate for describing ultrasonic degradation of schizophyllum polysaccharide [29] and dextran [24]. These findings can be attributed to the collapse of cavitation bubbles near the center of gravity of the polysaccharide molecule, resulting in the breaking of approach to the middle of molecular chains [24,30].

3.3. Effect of ultrasonic irradiation on the physicochemical properties

3.3.1. M_w, degradation degree and chemical composition

As shown in Fig. S3, HPLC chromatograph of PBP and the degraded polysaccharides (U-300, U-500 and U-700) contained single narrow elution peaks, demonstrating that these four polysaccharides were homogeneous fractions. Their physicochemical properties are presented in Table 2. Obviously, the M_w of the degraded polysaccharides decreased obviously with the increase of ultrasonic power, and the degradation rate of the polysaccharide at 700 W was 94.38%. Similarly, the M_w of *Phellinus linteus* mycelia decreased significantly with the increase of ultrasonic power intensities, and the M_w was reduced by 48.49% after treatment for 60 min under the ultrasonic power intensities of 453 W/cm^2 [12].

As shown in Table 2, the four polysaccharides had similar total sugar contents, while the degraded polysaccharides exhibited higher uronic acid contents compared to PBP. One possible explanation was that after ultrasonic treatment, more uronic acid inside the polysaccharide was exposed [32]. Moreover, the native polysaccharide and degraded polysaccharides were consisted of the same monosaccharide species (Fig. S4 and Table 2), and Ara, Rha and Gal were the major component in the four polysaccharides, suggesting ultrasound degradation did not affect the monosaccharide composition. However, slight differences in the monosaccharide molar ratios were observed among the four polysaccharides. Similarly, the polysaccharides from *Auricularia auricula* and *Ganoderma lucidum* before and after the ultrasonic degradation also had the same monosaccharide composition but different molar ratios [10,32].

Table 2
Physicochemical properties of PBP, U-300, U-500 and U-700.

Physicochemical properties	Samples			
	PBP	U-300	U-500	U-700
M_w (Da)	8.13×10^6	3.39×10^6	1.74×10^6	4.57×10^5
Degradation (%)		58.31%	78.62%	94.38%
Total sugar (%)	86.28 ± 0.36^a	87.30 ± 1.37^a	89.45 ± 0.32^b	88.68 ± 0.44^b
Uronic acid (%)	23.60 ± 0.27^a	27.32 ± 0.12^b	29.84 ± 0.24^c	31.24 ± 0.18^d
Monosaccharide (mol%)				
Rha	27.24	22.11	27.77	25.48
Ara	46.91	51.45	43.73	50.39
Man	3.81	3.96	5.59	3.84
Glc	4.18	4.21	7.39	3.19
Gal	17.86	18.27	15.52	17.10

Different letters in the same line indicate significant differences ($P < 0.05$).
Rha: rhamnose; Ara: arabinose; Man: mannose; Glc: glucose; Gal: galactose.

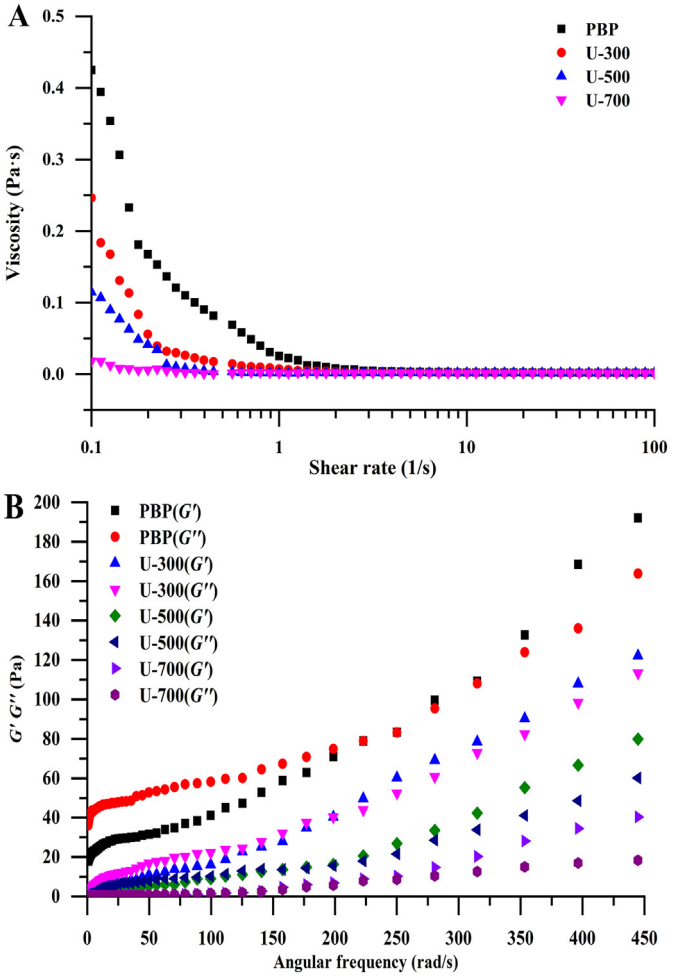


Fig. 3. (A) Effect of shear rate on the apparent viscosity of PBP and ultrasound-treated polysaccharides. (B) Storage modulus (G') and loss modulus (G'') of four polysaccharides.

3.3.2. Rheological properties

In general, polysaccharides with good rheological properties can be applied in food, biomedicine and other industries [33,34]. The steady

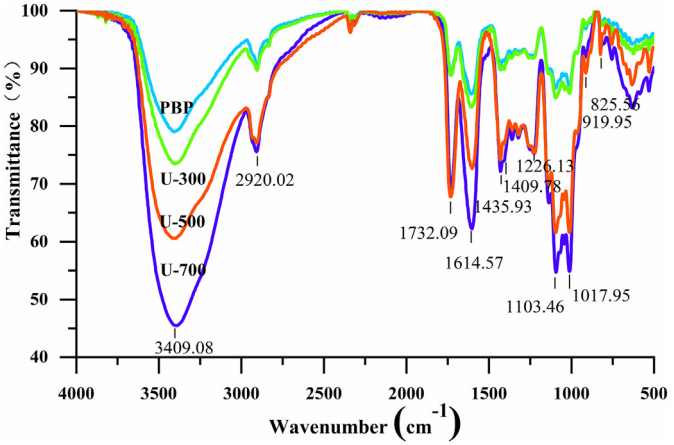


Fig. 4. FT-IR spectra of PBP and ultrasound-treated polysaccharides.

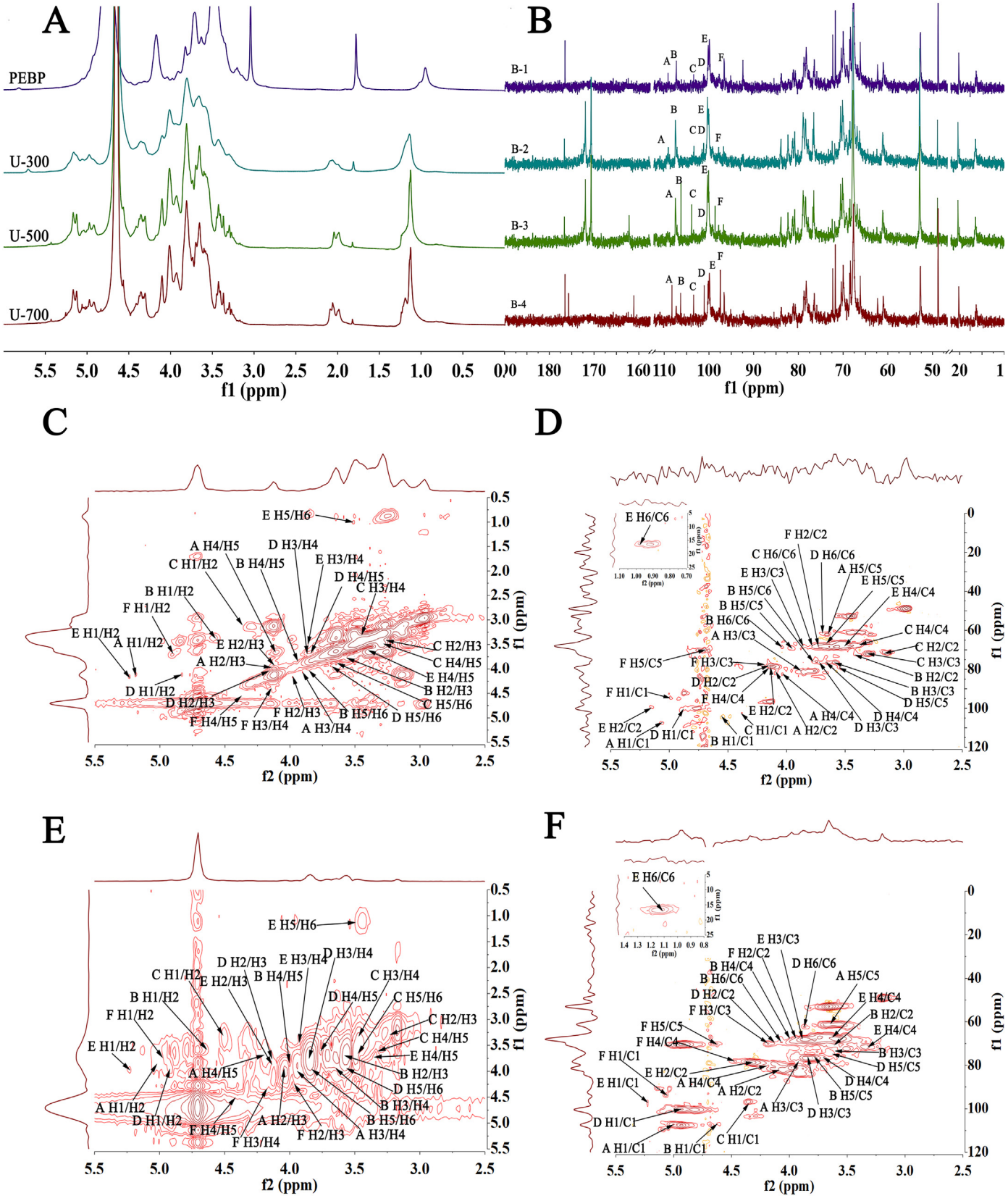


Fig. 5. The NMR spectra of PBP and ultrasound-treated polysaccharides in D_2O. (A) ^1H NMR spectra of PBP (A-1); U-300 (A-2); U-500 (A-3); and U-700 (A-4). (B) ^{13}C NMR spectra of PBP (B-1); U-300 (B-2); U-500 (B-3); and U-700 (B-4). 2D NMR spectra of U-700 (C, D) and PBP (E, F): (C, E) ^1H–^1H COSY; (D, F) ^1H–^{13}C HSQC.

shear flow curves of the polysaccharide solutions are described in Fig. 3A. PBP and two of the degraded polysaccharides (U-300 and U-500) exhibited both shear-thinning and Newtonian fluid behaviors depending on the shear rate. The shear-thinning behavior was indicated by the decreasing viscosity with increasing shear rate from 0.1 to 5 s^{-1}. However, at high shear rates (5–100 s^{-1}), near-Newtonian fluid

Table 3
^{1}H and ^{13}C NMR chemical shifts of H1/C1.

Samples	Chemical shifts of H1/C1 (ppm)					
PBP	5.05/107.20	4.63/106.12	4.46/104.15	4.92/101.09	5.29/99.88	4.97/96.62
U-300	5.16/109.16	4.55/107.11	4.35/103.37	4.87/101.16	5.24/100.26	4.97/97.82
U-500	5.16/107.53	4.56/106.30	4.42/103.88	4.85/100.33	5.23/99.98	4.97/97.62
U-700	5.17/108.29	4.57/106.37	4.41/103.54	4.82/101.03	5.26/99.50	4.99/97.45

behavior was observed, as indicated by the almost constant viscosity. Earlier reports suggested that flow directions of polysaccharides with long and disorderly chains tend to be aligned, thus polysaccharides chains are gradually disentangled as the shear rate increased, resulting in a Newtonian plateau at high shear rate [33,34]. Additionally, the apparent viscosity of U-700 was the lowest and remained almost constant with changing shear rate, indicating U-700 solution was close to the property of Newtonian fluid. It is probably explained that the breakage of the polysaccharides chains is strengthened with the power increase, and thus the intermolecular interactions are weakened, and the chain is difficultly entangled [31]. These results revealed the power of ultrasonic degradation led to remarkable changes in the rheological behavior of the polysaccharides from blackcurrant. Similarly, konjac glucomannan and apple pectin were also turned to Newtonian fluid under high ultrasonic power [28,31].

The changes in G' and G'' with angular frequency are illustrated in Fig. 3B. It could be observed that the G' and G'' values of all four polysaccharides increased with increasing angular frequency, and both G' and G'' were lower for the degraded polysaccharides than for PBP. As presented in Fig. 4B, both the degraded polysaccharides and PBP solutions were viscoelastic fluids, which displayed liquid-like behavior ($G'' > G'$) in the low-frequency region, and weak gel behavior ($G'' < G'$) in the high-frequency region. Similar results were obtained for the polysaccharides from *Rosa roxburghii Tratt* [33]. Moreover, the crossover angular frequencies of the four polysaccharides presented at 229.94 (PBP), 198.69 (U-300), 157.83 (U-500) and 125.37 rad/s (U-700), separately. Obviously, crossover frequencies of the degraded polysaccharides were lower than that of PBP, and decreased with increasing power. A low crossover frequency is thought to indicate good gelling character and system stability [35]. Thus, compared to PBP, the degraded polysaccharides possessed better rheological properties, and may be used in the food industry [33].

3.3.3. FT-IR analysis

As shown in Fig. 4, the FT-IR spectra of the polysaccharides before and after ultrasonic treatment were nearly identical. The absorption bands at 3409.08, 2920.02 and 1732.09 cm^{-1} belonged to O—H, C—H and C═O stretching vibration, respectively [7]. The peaks appeared at 1614.57 and 1435.93 cm^{-1} confirmed the existence of free forms (non-esterified) of carboxylic group ($-COO^{-}$) [12,35]. The presence of pyranose ring was supported by the absorption bands at 1103.46 and 1017.95 cm^{-1} [33,36]. The characteristic absorption bands at 919.95 and 825.56 cm^{-1} indicated simultaneous existence of α- and β-glycosidic bonds [7,33]. These results indicated that the ultrasonic degradation did not change the characteristic organic groups of the polysaccharides.

3.3.4. NMR analysis

NMR spectroscopy was applied to interpret the structural features of PBP before and after ultrasonic treatment. As observed in Fig. 5A–B, the ^{1}H and ^{13}C NMR spectra of U-300, U-500 and U-700 were similar to those of PBP. The chemical shifts of typical peaks appeared in δ_H 4.0–5.5 and δ_C 90.0–110.0, suggesting the existence of both α-and β-anomeric configurations in the four polysaccharides [6]. In addition, six signal peaks in the anomeric region were observed, respectively (data shown in Table 3). Obviously, the signals were almost the same in the four polysaccharides, implying the existence of the same glycosidic linkage patterns. The six main glycosyl types belonged to α-L-Ara*f*, β-D-Gal*p*, β-D-Glc*p*, β-D-Man*p*, α-L-Rha*p* and α-D-GalA*p* [37–41]. Moreover, the significant signal at approximately δ 176 was attributed to C-6 galacturonic acid residues [40,41].

To provide detailed structural information of the polysaccharides, the 2D NMR (COSY and HSQC) spectra of U-700 and PBP are displayed in Fig. 5C–F. According to the 2D NMR spectra and the published references, U-700 and PBP had the same six types of glycosidic linkage patterns, which were confirmed as α-L-Ara*f*-(1→, →6)-β-D-Gal*p*-(1→, →3,6)-β-D-Glc*p*-(1→, →4)-β-D-Man*p*-(1→, →2)-α-L-Rha*p*-(1→, and →4)-α-D-GalA*p*-(1→ (the chemical shifts are shown in Table 4). These results demonstrated that ultrasonic treatment did not change the main chain structure of blackcurrant polysaccharides.

3.4. Effect of the polysaccharides on erythrocyte hemolysis

Erythrocytes are the most common blood cells that transport oxygen to body tissues via the blood. However, erythrocytes are highly susceptible to oxidative damage because of the high content of oxygen, hemoglobin (Hb), and membrane polyunsaturated fatty acid [42,43]. Hydrogen peroxide (H_2O_2), as an important reactive oxygen species (ROS), can easily cross cell membrane, and react with Hb to product reactive radical species. Then these radical species will react immediately

Table 4
^{1}H and ^{13}C NMR chemical shifts of $^{1}H/^{13}C$. (A–F) U-700; (A′–F′) PBP.

Sugar residues		Chemical shifts of $^{1}H/^{13}C$ (ppm)						References
		1	2	3	4	5	6	
α-L-Ara*f*-(1→	A	5.13/108.29	4.10/82.15	3.88/79.45	4.03/82.77	3.67/62.20	–	[39,41]
	A′	5.05/107.20	4.07/83.45	3.89/77.93	4.16/82.78	3.66/61.27	–	
→6)-β-D-Gal*p*-(1→	B	4.57/106.37	3.50/72.87	3.66/73.65	3.94/69.27	3.88/76.01	4.01/69.03	[39]
	B′	4.63/106.12	3.59/72.07	3.66/72.24	3.97/69.20	3.83/75.11	4.02/70.36	
→3,6)-β-D-Glc*p*-(1→	C	4.41/103.54	3.21/72.31	3.40/84.52	3.33/68.55	3.52/76.44	3.73/70.1	[40]
	C′	4.46/104.15	3.28/72.85	3.42/82.96	3.36/69.75	3.52/73.80	3.66/70.69	
→4)-β-D-Man*p*-(1→	D	4.82/101.03	4.10/74.50	3.88/76.21	3.78/76.03	3.56/77.60	3.73/62.02	[37]
	D′	4.92/101.09	4.10/71.46	3.87/75.64	3.77/76.72	3.58/77.26	3.89/62.61	
→2)-α-L-Rha*p*-(1→	E	5.26/99.50	4.10/78.6	3.87/68.60	3.45/73.01	3.66/68.12	1.06/16.50	[38,39]
	E′	5.29/99.88	4.10/77.93	3.89/68.56	3.34/72.27	3.61/68.20	1.12/16.58	
→4)-α-D-GalA*p*-(1→	F	4.99/97.45	3.83/69.37	4.13/74.50	4.38/78.69	4.57/72.31	176.49	[38,39]
	F′	4.97/96.62	3.90/69.16	4.12/74.60	4.45/78.31	4.65/71.04	176.48	

with anything in vicinity, and eventually lead to the oxidative stress on erythrocyte membrane [42]. Therefore, H_2O_2 is often used to induce oxidative stress in vitro to assess oxidative damage on erythrocyte.

3.4.1. Protective effects of the polysaccharides against erythrocyte hemolysis

As shown in Fig. 6A, the protective effects of both the polysaccharides and Trolox against the H_2O_2-induced erythrocyte hemolysis were concentration-dependent ($P < 0.05$). The highest inhibitory rates of PBP, U-300, U-500, U-700 and Trolox were 60.58% ± 0.52%, 67.73% ± 0.18%, 70.22% ± 0.62%, 76.24% ± 0.71% and 59.82% ± 1.09%, respectively, at a dose of 4.0 mg/mL. In addition, three ultrasound-treated polysaccharides exerted higher inhibitory activities than PBP and Trolox, and the inhibitory rate increased with increasing ultrasonic power at tested concentrations (1.0–4.0 mg/mL). Those results confirmed the degraded (low-molecular-weight) polysaccharides from blackcurrant fruits possessed high inhibitory effects against H_2O_2-induced erythrocyte hemolysis.

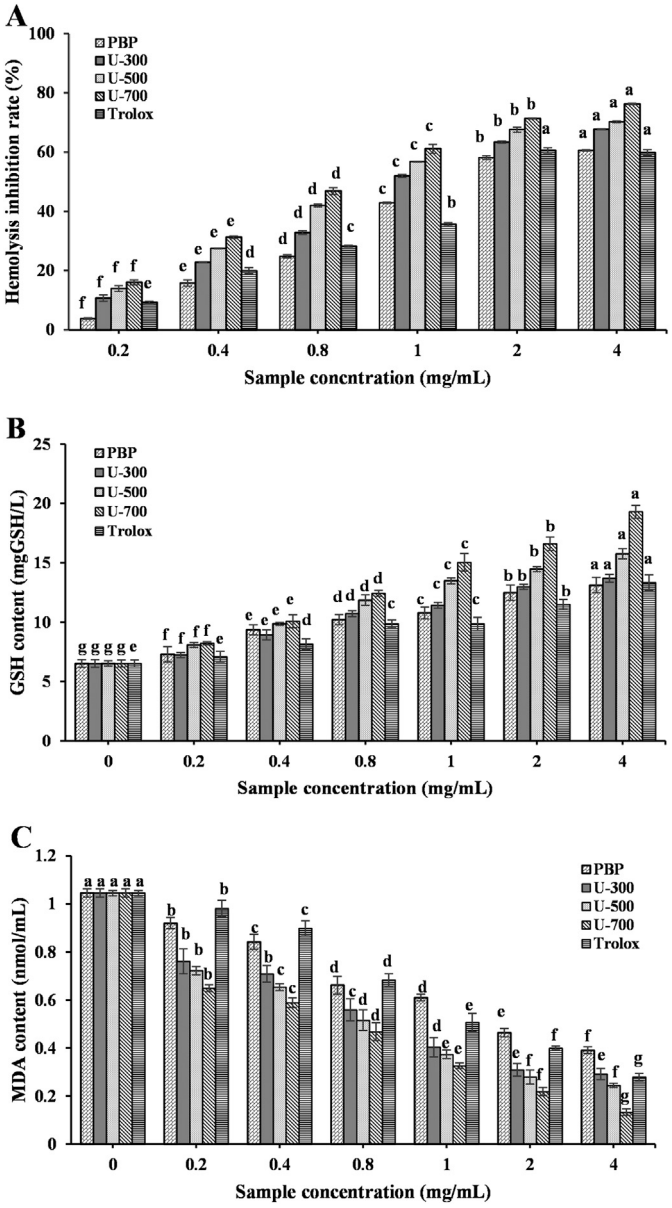


Fig. 6. Effects of the polysaccharides on hemolysis inhibition (A), GSH levels (B) and MDA levels (C) in H_2O_2-induced erythrocytes (the means with different letter significantly differ, $P < 0.05$).

3.4.2. Effects of the polysaccharides on GSH contents of erythrocytes

GSH is a major antioxidant that plays an important role in protecting cells against oxidative stress. Thus, the depletion of GSH is used as an indicator of intracellular oxidation [18,43]. As could been seen from Fig. 6B, the contents of GSH in all samples increased in a concentration-dependent manner (0.2–4.0 mg/mL, $P < 0.05$). In addition, all the degraded polysaccharides showed higher levels of GSH than PBP and Trolox in the concentration range of 0.4–4.0 mg/mL. The increase of GSH content was well correlated with raising ultrasonic power at all tested concentrations. At the highest tested concentration of 4.0 mg/mL, GSH contents were 13.12 ± 0.33 for PBP, 13.69 ± 0.33 for U-300, 15.75 ± 0.43 for U-500, 19.29 ± 0.54 for U-700 and 13.33 ± 0.65 mg GSH/L for Trolox, respectively. The results demonstrated that the degraded polysaccharides with lower M_w displayed the better effect on preventing intracellular oxidation.

3.4.3. Effects of the polysaccharides on MDA generation

MDA is a vital end product of lipid peroxidation that can damage the structure and function of the cell membrane, and seriously influence the cellular metabolism [44]. Therefore, the content of MDA is considered as an important index to reflect the degree of lipid peroxidation or even identify damage the cell membrane [18,44]. MDA contents of all samples are presented in Fig. 6C. It was observed that MDA contents significantly decreased with increasing tested samples concentrations (0.2–4.0 mg/mL, $P < 0.05$). Moreover, the inhibitory effects of the degraded polysaccharides on MDA formation were stronger than those of PBP and Trolox, and the inhibitory effects increased with the increment of the ultrasonic power. At the highest test concentration (4.0 mg/mL), MDA contents reached the lowest point, and the reduced degrees of PBP, U-300, U-500, U-700 and Trolox were 62.55% ± 1.88%, 72.00% ± 3.20%, 76.52% ± 1.70%, 87.26% ± 1.69% and 73.22% ± 2.36% respectively, compared to the test group without polysaccharides.

Based on the above results, the degraded polysaccharides displayed better protective effects against H_2O_2-induced erythrocyte hemolysis than the untreated polysaccharides and Trolox. Notably, U-700, which had the lowest molecular weight exerted the strongest antioxidant activity among all tested samples, demonstrating molecular weight is be one of the critical factors for the antioxidant capacity of the polysaccharides [10,13]. Previous studies suggest that ultrasonic degradation exposes more active OH groups located in the inner core of the polysaccharides, and OH groups can eliminate ROS to reduce oxidative damage [45]. In addition, a high level of acidic monosaccharide is beneficial for antioxidant activity [10,13,36]. In this study, the degraded polysaccharides possessed higher content of uronic acid than PBP, contributing to antioxidative effects of these polysaccharides.

4. Conclusion

The ultrasonic degradation of blackcurrant polysaccharides was found to adhere to second-order kinetics model and midpoint chain scission model. The principal structure of the degraded polysaccharides (U-300, U-500 and U-700) was not significantly different from that of the native polysaccharide. After ultrasonic treatment, three degraded polysaccharides exhibited excellent rheological properties along with stronger protective effects against erythrocyte hemolysis compared to the native polysaccharide. Therefore, ultrasonic radiation is a feasible technique for preparing the functional polysaccharides with low M_w.

CRediT authorship contribution statement

Haihong Yang and Jingwen Bai performed the experiments, and drafted the manuscript. Conglei Ma conducted some physicochemical properties analysis. Libo Wang assisted in conducting the ultrasound degradation, guided and elaborated the data of 1D/2D NMR. Xiaoqing Li and Yu Zhang performed activity experiments. Yaqin Xu and Yu Yang designed experiments and polished the English writing.

Declaration of competing interest

No conflict of interest exits in the submission of this manuscript.

Acknowledgement

This work was financially supported by National Natural Science Foundation of China (NO. 31600276), Natural Science Foundation of Heilongjiang Province of China (NO. C2018013) and Student's Innovation Training Program of Heilongjiang Province of China (NO. 202010224032).

Ethic statement

The protocol for this experiment was approved by the ethics committee of Harbin Veterinary Research Institute at the Chinese Academy of Agricultural Sciences (SYXK (Hei) 2012-2067).

Appendix A. Supplementary data

Supplementary data to this article can be found online at https://doi.org/10.1016/j.ijbiomac.2020.09.093.

References

[1] H. Ashigai, Y. Komano, G. Wang, Y. Kawachi, K. Sunaga, R. Yamamoto, R. Takata, M. Miyake, T. Yana, Effect of administrating polysaccharide from black currant (*Ribes nigrum* L.) on atopic dermatitis in NC/Nga mice, Biosci. Microbiota. Food Health 37 (1) (2018) 19–24.
[2] R.E. Cortez, E. Gonzalez de Mejia, Blackcurrants (*Ribes nigrum*): a review on chemistry, processing, and health benefits, J. Food Sci. 84 (9) (2019) 2387–2401.
[3] S.K. Barik, W.R. Russell, K.M. Moar, M. Cruickshank, L. Scobbie, G. Duncan, N. Hoggard, The anthocyanins in black currants regulate postprandial hyperglycaemia primarily by inhibiting alpha-glucosidase while other phenolics modulate salivary alpha-amylase, glucose uptake and sugar transporters, J. Nutr. Biochem. 78 (2020) 108325.
[4] P. Strugała, W. Gładkowski, A.Z. Kucharska, A. Sokół-Łętowska, J. Gabrielska, Antioxidant activity and anti-inflammatory effect of fruit extracts from blackcurrant, chokeberry, hawthorn, and rosehip, and their mixture with linseed oil on a model lipid membrane, Eur. J. Lipid Sci. Technol. 118 (3) (2016) 461–474.
[5] Y.Q. Xu, Y.Y. Guo, S.Y. Duan, H. Wei, Y.S. Liu, L.B. Wang, X. Huo, Y. Yang, Effects of ultrasound irradiation on the characterization and bioactivities of the polysaccharide from blackcurrant fruits, Ultrason. Sonochem. 49 (2018) 206–214.
[6] Y.Q. Xu, G.J. Liu, Z.Y. Yu, X.M. Song, X.G. Li, Y. Yang, L.B. Wang, L. Liu, J. Dai, Purification, characterization and antiglycation activity of a novel polysaccharide from black currant, Food Chem. 199 (2016) 694–701.
[7] Y.Q. Xu, X.J. Niu, N.Y. Liu, Y.K. Gao, L.B. Wang, G. Xu, X.G. Li, Y. Yang, Characterization, antioxidant and hypoglycemic activities of degraded polysaccharides from blackcurrant (*Ribes nigrum* L.) fruits, Food Chem. 243 (2018) 26–35.
[8] S.J. Li, Q.P. Xiong, X.P. Lai, X. Li, M.J. Wan, J.N. Zhang, Y.J. Yan, M. Cao, L. Lu, J.M. Guan, Molecular modification of polysaccharides and resulting bioactivities, Compr. Rev. Food Sci. Food Saf. 15 (2) (2016) 237–250.
[9] J.H. Li, S. Li, Y.F. Zheng, H. Zhang, J.L. Chen, L.F. Yan, T. Ding, R.J. Linhardt, C. Orfila, D.H. Liu, X.Q. Ye, S.G. Chen, Fast preparation of rhamnogalacturonan I enriched low molecular weight pectic polysaccharide by ultrasonically accelerated metal-free Fenton reaction, Food Hydrocoll. 95 (2019) 551–561.
[10] J.Q. Qiu, H. Zhang, Z.Y. Wang, Ultrasonic degradation of polysaccharides from *Auricularia auricula* and the antioxidant activity of their degradation products, LWT Food Sci. Technol. 113 (2019) 108266.
[11] F.M. Ma, J.W. Wu, P. Li, D.B. Tao, H.T. Zhao, B.Q. Zhang, B. Li, Effect of solution plasma process with hydrogen peroxide on the degradation of water-soluble polysaccharide from *Auricularia auricula*. II: solution conformation and antioxidant activities in vitro, Carbohydr. Polym. 198 (2018) 575–580.
[12] J.K. Yan, Y.Y. Wang, H.L. Ma, Z.B. Wang, Ultrasonic effects on the degradation kinetics, preliminary characterization and antioxidant activities of polysaccharides from *Phellinus linteus* mycelia, Ultrason. Sonochem. 29 (2016) 251–257.
[13] H. Zhang, X.T. Cai, Q.H. Tian, L.X. Xiao, Z. Zeng, X.T. Cai, J.Z. Yan, Q.Y. Li, Microwave-assisted degradation of polysaccharide from *Polygonatum sibiricum* and antioxidant activity, J. Food Sci. 84 (4) (2019) 754–761.
[14] P.S. Saravana, Y.N. Cho, M.P. Patil, Y.J. Cho, G.D. Kim, Y.B. Park, H.C. Woo, B.S. Chun, Hydrothermal degradation of seaweed polysaccharide: characterization and biological activities, Food Chem. 268 (2018) 179–187.
[15] L.N. Ren, X.F. Wang, S. Li, J.L. Li, X.D. Zhu, L. Zhang, F. Gao, G.H. Zhou, Effect of gamma irradiation on structure, physicochemical and immunomodulatory properties of *Astragalus* polysaccharides, Int. J. Biol. Macromol. 120 ((2018) 641–649.
[16] X. Guo, X.Q. Ye, Y.J. Sun, D. Wu, N. Wu, Y.Q. Hu, S.G. Chen, Ultrasound effects on the degradation kinetics, structure, and antioxidant activity of sea cucumber fucoidan, J. Agric. Food Chem. 62 (5) (2014) 1088–1095.
[17] Z.J. Wang, J.H. Xie, S.P. Nie, M.Y. Xie, Review on cell models to evaluate the potential antioxidant activity of polysaccharides, Food Funct. 8 (3) (2017) 915–926.
[18] W.B. Chen, J.J. Ma, F. Gong, H.R. Xi, Q.P. Zhan, X.F. Li, F.S. Wei, H. Wu, F.R. Lai, Two novel polysaccharides from the torus of *Saussurea laniceps* protect against AAPH-induced oxidative damage in human erythrocytes, Carbohydr. Polym. 200 (2018) 446–455.
[19] A.L. Prajapat, P.R. Gogatedifferent, Depolymerization of guar gum solution using different approaches based on ultrasound and microwave irradiations, Chem. Eng. Process. 88 (2015) 1–9.
[20] R.J. Young, P.A. Lovell, Introduction to Polymers, 2nd ed. Chapman and Hall, New York, 1991.
[21] K. Zhong, Q. Zhang, L.T. Tong, L.Y. Liu, X.R. Zhou, S.M. Zhou, Molecular weight degradation and rheological properties of schizophyllan under ultrasonic treatment, Ultrason. Sonochem. 23 (2015) 75–80.
[22] T. Wu, S. Zivanovic, D.G. Hayes, J. Weiss, Efficient reduction of chitosan molecular weight by high-intensity ultrasound: underlying mechanism and effect of process parameters, J. Agric. Food Chem. 56 (13) (2008) 5112–5119.
[23] M. Dubois, K.A. Gilles, J.K. Hamilton, P.A. Rebers, F. Smith, Colorimetric method for determination of sugars and related substances, Anal. Chem. 28 (3) (1956) 350–356.
[24] Y.Y. Pu, Q.S. Zou, D.Z. Hou, Y.P. Zhang, S. Chen, Molecular weight kinetics and chain scission models for dextran polymers during ultrasonic degradation, Carbohydr. Polym. 156 (2017) 71–76.
[25] P.K. Kintner, J.P. Van Buren, Carbohydrate interference and its correction in pectin analysis using the m-hydroxydiphenyl method, J. Food Sci. 47 (1982) 756–759.
[26] G.X. Ma, W.J. Yang, A.M. Mariga, Y. Fang, N. Ma, F. Pei, Purification, characterization and antitumor activity of polysaccharides from *Pleurotus eryngii* residue, Carbohydr. Polym. 114 (2014) 297–305.
[27] S.Y. Duan, M.M. Zhao, B.Y. Wu, S.J. Wang, Y. Yang, Y.Q. Xu, L.B. Wang, Preparation, characteristics, and antioxidant activities of carboxymethylated polysaccharides from blackcurrant fruits, Int. J. Biol. Macromol. 155 (2020) 1114–1122.
[28] L.F. Zhang, X.Q. Ye, T. Ding, X.Y. Sun, Y.T. Xu, D.H. Liu, Ultrasound effects on the degradation kinetics, structure and rheological properties of apple pectin, Ultrason. Sonochem. 20 (1) (2013) 222–231.
[29] T. Yanaki, K. Nishii, K. Tabata, T. Kojima, Ultrasonic degradation of *Schizophyllum Commune* polysaccharide in dilute aqueous solution, J. Appl. Polym. Sci. 28 (1983) 873–878.
[30] T. Poinot, K. Benyahia, A. Govin, T. Jeanmaire, P. Grosseau, Use of ultrasonic degradation to study the molecular weight influence of polymeric admixtures for mortars, Constr. Build. Mater. 47 (2013) 1046–1052.
[31] J. Li, B. Li, P. Geng, A.X. Song, J.Y. Wu, Ultrasonic degradation kinetics and rheological profiles of a food polysaccharide (konjac glucomannan) in water, Food Hydrocoll. 70 (2017) 14–19.
[32] Y. Xu, X. Zhang, X.H. Yan, J.L. Zhang, L.Y. Wang, H. Xue, G.C. Jiang, X.T. Ma, X.J. Liu, Characterization, hypolipidemic and antioxidant activities of degraded polysaccharides from *Ganoderma lucidum*, Int. J. Biol. Macromol. 135 (2019) 706–716.
[33] L. Wang, B. Zhang, J. Xiao, Q. Huang, C. Li, X. Fu, Physicochemical, functional, and biological properties of water-soluble polysaccharides from *Rosa roxburghii Tratt* fruit, Food Chem. 249 (2018) 127–135.
[34] S.N. Wang, L.L. Zhao, Q.H. Li, C. Liu, J.L. Han, L.J. Zhu, D.S. Zhu, Y.T. He, H. Liu, Rheological properties and chain conformation of soy hull water-soluble polysaccharide fractions obtained by gradient alcohol precipitation, Food Hydrocoll. 91 (2019) 34–39.
[35] J. Gao, L.Z. Lin, B.G. Sun, M.M. Zhao, A comparison study on polysaccharides extracted from *Laminaria japonica* using different methods: structural characterization and bile acid-binding capacity, Food Funct. 8 (9) (2017) 3043–3052.
[36] G.J. Chen, F. Bu, X.H. Chen, C.F. Li, S.S. Wang, J.Q. Kan, Ultrasonic extraction, structural characterization, physicochemical properties and antioxidant activities of polysaccharides from bamboo shoots (*Chimonobambusa quadrangularis*) processing by-products, Int. J. Biol. Macromol. 112 (2018) 656–666.
[37] M. Beigi, K. Jahanbin, A water-soluble polysaccharide from the roots of *Eremurus spectabilis* M. B. subsp. *spectabilis*: extraction, purification and structural features, Int. J. Biol. Macromol. 128 (2019) 648–654.
[38] J.W. Choi, A. Synytsya, P. Capek, R. Bleha, R. Pohl, Y.I. Park, Structural analysis and anti-obesity effect of a pectic polysaccharide isolated from Korean mulberry fruit Oddi (*Morus alba* L.), Carbohydr. Polym. 146 (2016) 187–196.
[39] J. Liu, Y.P. Zhao, Q.X. Wu, A. John, Y.M. Jiang, J.L. Yang, H.L. Liu, B. Yang, Structure characterisation of polysaccharides in vegetable "okra" and evaluation of hypoglycemic activity, Food Chem. 242 (2018) 211–216.
[40] K.C. Siu, L.J. Xu, X. Chen, J.Y. Wu, Molecular properties and antioxidant activities of polysaccharides isolated from alkaline extract of wild *Armillaria ostoyae* mushrooms, Carbohydr. Polym. 137 (2016) 739–746.
[41] L. Xia, Deji, M.X. Zhu, D.F. Chen, Y. Lu, *Juniperus pingii var. wilsonii* acidic polysaccharide: extraction, characterization and anticomplement activity, Carbohydr. Polym. 231 (2020) 115728.
[42] J.J. van den Berg, J.A. Op den Kamp, B.H. Lubin, B. Roelofsen, F.A. Kuypers, Kinetics and site specificity of hydroperoxide-induced oxidative damage in red blood cells, Free Radical Biol. Med. 12 (1992) 487–498.
[43] H.L. Yang, M. Korivi, M.K. Lin, H.C. Chang, C.R. Wu, M.S. Lee, W.T. Chen, Y.C. Hseu, Antihemolytic and antioxidant properties of pearl powder against 2,2′-azobis (2-amidinopropane) dihydrochloride-induced hemolysis and oxidative damage to erythrocyte membrane lipids and proteins, J. Food Drug Anal. 25 (4) (2017) 898–907.
[44] W. Liao, L. Chen, B. Yu, Z. Lei, X. Wu, J. Yang, J. Ren, Cell-based evaluation of a novel *Dictyophora indusiata* polysaccharide against oxidative-induced erythrocyte hemolysis, Cell. Mol. Biol. 62 (1) (2016) 38–44.
[45] I. Rjeibi, A. Feriani, F. Hentati, N. Hfaiedh, P. Michaud, G. Pierre, Structural characterization of water-soluble polysaccharides from Nitraria retusa fruits and their antioxidant and hypolipidemic activities, Int. J. Biol. Macromol. 129 (2019) 422–432.